

Near-infrared polarimetry of the GG Tauri A binary system

This content has been downloaded from IOPscience. Please scroll down to see the full text.

[View the table of contents for this issue](#), or go to the [journal homepage](#) for more

Download details:

IP Address: 198.119.56.43

This content was downloaded on 09/02/2015 at 17:04

Please note that [terms and conditions apply](#).

Near-infrared polarimetry of the GG Tauri A binary system [∗]

Yoichi Itoh¹, Yumiko Oasa², Tomoyuki Kudo³, Nobuhiko Kusakabe⁴, Jun Hashimoto⁵,
Lyu Abe⁶, Wolfgang Brandner⁷, Timothy D. Brandt⁸, Joseph C. Carson⁹, Sebastian
Egner³, Markus Feldt⁹, Carol A. Grady^{10,11,12}, Olivier Guyon³, Yutaka Hayano³,
Masahiko Hayashi⁴, Saeko S. Hayashi³, Thomas Henning⁷, Klaus W. Hodapp¹³,
Miki Ishii³, Masanori Iye⁴, Markus Janson⁸, Ryo Kandori⁴, Gillian R. Knapp⁸,
Masayuki Kuzuhara¹⁴, Jungmi Kwon⁴, Taro Matsuo¹⁵, Michael W. McElwain¹⁰,
Shoken Miyama¹⁶, Jun-Ichi Morino⁴, Amaya Moro-Martin^{8,17}, Tetsuo Nishimura³,
Tae-Soo Pyo³, Eugene Serabyn¹⁸, Takuya Suenaga^{4,19}, Hiroshi Suto⁴, Ryuji Suzuki⁴,
Yasuhiro H. Takahashi^{20,4}, Naruhisa Takato³, Hiroshi Terada³, Christian Thalmann²¹,
Daigo Tomono³, Edwin L. Turner^{8,22}, Makoto Watanabe²³, John Wisniewski⁵,
Toru Yamada²⁴, Satoshi Mayama²⁵, Thayne Currie²⁶, Hideki Takami⁴,
Tomonori Usuda⁴, Motohide Tamura^{20,4}

¹ Nishi-Harima Astronomical Observatory, Center for Astronomy, University of Hyogo, 407-2, Nishigaichi, Sayo, Hyogo 679-5313, Japan; yitoh@nhao.jp

² Faculty of Education, Saitama University, 255 Shimo-Okubo, Sakura, Saitama, Saitama 338-8570, Japan

³ Subaru Telescope, National Astronomical Observatory of Japan, 650 North A'ohoku Place, Hilo, HI 96720, USA

⁴ National Astronomical Observatory of Japan, 2-21-1, Osawa, Mitaka, Tokyo, 181-8588, Japan

⁵ H.L. Dodge Department of Physics & Astronomy, University of Oklahoma, 440 W Brooks St. Norman, OK 73019, USA

⁶ Laboratoire Lagrange (UMR 7293), Université de Nice-Sophia Antipolis, CNRS, Observatoire de la Côte d'Azur, 28 avenue Valrose, 06108 Nice Cedex 2, France

⁷ Max Planck Institute for Astronomy, Königstuhl 17, 69117 Heidelberg, Germany

⁸ Department of Astrophysical Science, Princeton University, Peyton Hall, Ivy Lane, Princeton, NJ 08544, USA

⁹ Department of Physics and Astronomy, College of Charleston, 58 Coming St., Charleston, SC 29424, USA

¹⁰ Exoplanets and Stellar Astrophysics Laboratory, Code 667, Goddard Space Flight Center, Greenbelt, MD 20771, USA

¹¹ Eureka Scientific, 2452 Delmer, Suite 100, Oakland CA 94602, USA

¹² Goddard Center for Astrobiology, Greenbelt, MD 20771, USA

¹³ Institute for Astronomy, University of Hawaii, 640 N. Aohoku Place, Hilo, HI 96720, USA

¹⁴ Department of Earth and Planetary Sciences, Tokyo Institute of Technology, Ookayama, Meguro-ku, Tokyo 152-8551, Japan

¹⁵ Department of Astronomy, Kyoto University, Kitashirakawa-Oiwake-cho, Sakyo-ku, Kyoto, Kyoto 606-8502, Japan

[∗] Based on data collected at the Subaru Telescope, which is operated by the National Astronomical Observatory of Japan.

- ¹⁶ Hiroshima University, 1-3-2, Kagamiyama, Higashihiroshima, Hiroshima 739-8511, Japan
- ¹⁷ Department of Astrophysics, CAB-CSIC/INTA, 28850 Torrejón de Ardoz, Madrid, Spain
- ¹⁸ Jet Propulsion Laboratory, California Institute of Technology, Pasadena, CA, 91109, USA
- ¹⁹ Department of Astronomical Science, The Graduate University for Advanced Studies, 2-21-1, Osawa, Mitaka, Tokyo, 181-8588, Japan
- ²⁰ Department of Astronomy, The University of Tokyo, 7-3-1, Hongo, Bunkyo-ku, Tokyo, 113-0033, Japan
- ²¹ Astronomical Institute “Anton Pannekoek”, University of Amsterdam, Postbus 94249, 1090 GE, Amsterdam, The Netherlands
- ²² Kavli Institute for Physics and Mathematics of the Universe, The University of Tokyo, 5-1-5, Kashiwanoha, Kashiwa, Chiba 277-8568, Japan
- ²³ Department of Cosmosciences, Hokkaido University, Kita-ku, Sapporo, Hokkaido 060-0810, Japan
- ²⁴ Astronomical Institute, Tohoku University, Aoba-ku, Sendai, Miyagi 980-8578, Japan
- ²⁵ The Center for the Promotion of Integrated Sciences, The Graduate University for Advanced Studies (SOKENDAI), Shonan International Village, Hayama-cho, Miura-gun, Kanagawa 240-0193, Japan
- ²⁶ Department of Astronomy & Astrophysics, University of Toronto, 50 George St., Toronto, Ontario, M5S 3H4, Canada

Received 2013 November 29; accepted 2014 May 4

Abstract A high angular resolution near-infrared image that shows the intensity of polarization for the GG Tau A binary system was obtained with the Subaru Telescope. The image shows a circumbinary disk scattering the light from the central binary. The azimuthal profile of the intensity of polarization for the circumbinary disk is roughly reproduced by a simple disk model with the Henyey-Greenstein phase function and the Rayleigh function, indicating there are small dust grains at the surface of the disk. Combined with a previous observation of the circumbinary disk, our image indicates that the gap structure in the circumbinary disk orbits counterclockwise, but material in the disk orbits clockwise. We propose that there is a shadow caused by material located between the central binary and the circumbinary disk. The separations and position angles of the stellar components of the binary in the past 20 yr are consistent with the binary orbit with $a = 33.4$ AU and $e = 0.34$.

Key words: stars: individual (GG Tauri) — stars: pre-main sequence — techniques: high angular resolution

1 INTRODUCTION

Proto-planetary disks are common structures around classical T Tauri stars. A number of disks have been investigated at various wavelengths. However, many observations have focused on the disks around single stars, but more than half of T Tauri stars are binaries (Ghez et al. 1993; Leinert et al. 1993). Disks around binaries are expected to have forms different from those around single stars. Artymowicz & Lubow (1996) indicated that there are two kinds of disks around a binary system: a circumstellar disk associated with each star and a ring-shaped circumbinary disk around the binary system. A cavity exists between the circumbinary disk and the central binary. Several circumbinary disks have been spatially resolved at near-infrared wavelengths (e.g. UY Aur, Hioki et al. 2007; FS Tau, Hioki et al. 2011).

GG Tau ($d \sim 140$ pc) is a well-studied young multiple system. The system has two binaries: GG Tau Aa/Ab and GG Tau Ba/Bb. The GG Tau A binary (hereafter GG Tau) is especially interesting, because its circumbinary disk has been spatially resolved at millimeter wavelengths (Guilloteau et al. 1999), at near-infrared (Roddier et al. 1996; Itoh et al. 2002), and at optical (Krist et al. 2002). The large-scale structure of the circumbinary disk is well characterized by an annulus with an inner radius of 190 AU. The disk is inclined by $\sim 37^\circ$ with the northern edge nearest to us. The kinematics of the disk are consistent with clockwise Keplerian rotation (Guilloteau et al. 1999). Duchêne et al. (2004) observed GG Tau at the L' -band ($\lambda = 3.8$ μm). Comparing this with shorter wavelength images, they proposed a stratified structure for the circumbinary disk, in which large dust grains are present near the disk's midplane. They suggested that there is vertical dust settling and grain growth in the dense part of the disk.

Polarimetric observations also yield insight into dust properties and disk structures. Tanii et al. (2012) carried out near-infrared polarimetry for UX Tau. The circumstellar disk of UX Tau shows a large variety in the degree of polarization, from 1.6% up to 66%. They attributed this large variation to large non-spherical dust grains in the circumstellar disk. This observation confirmed that there can be dust growth in a circumstellar disk. On the other hand, several observations have suggested that there are small dust grains in proto-planetary disks. Silber et al. (2000) carried out polarimetric observations of GG Tau at 1 μm . They found that the circumbinary disk is strongly polarized, up to $\sim 50\%$, which is indicative of Rayleigh-like scattering from sub-micron dust grains.

We present the results of near-infrared polarimetry of GG Tau. Combining a coronagraph with an adaptive optics (AO) system, we obtained a high spatial resolution image of GG Tau that shows the intensity of polarization. The observations and the data-reduction procedure are described in Section 2. In Section 3, we discuss the circumbinary structures around GG Tau and the orbital motion of the GG Tau binary. Conclusions are given in Section 4.

2 OBSERVATIONS AND DATA REDUCTION

Near-infrared H -band (1.6 μm) polarimetric imaging observations of GG Tau A were acquired on 2011 September 4 with the High Contrast Instrument for the Subaru next-generation Adaptive Optics (HiCIAO) and the AO system, AO188 mounted on the Nasmyth platform of the Subaru Telescope. The observations were conducted as part of the SEEDS survey. We employed the Polarization Differential Imaging (PDI) mode. In this mode, the Wollaston prism installed in HiCIAO divides the incident light into two linearly polarized components, which are perpendicular to each other and imaged simultaneously on the detector. Each image has 1024×2048 pixels with a field of view of $9.75'' \times 20.09''$ and a pixel scale of 9.521 mas pixel^{-1} in the east-west direction and 9.811 mas pixel^{-1} in the north-south direction. In the PDI mode, when the half-wave plate is set at an offset angle of 0° , 45° , 22.5° and 67.5° , we obtain polarimetric images with polarization directions at 0° and 90° , 90° and 0° , 45° and 135° , and 135° and 45° components, respectively. The full width at half maximum of the point spread function (PSF) was $0.11''$. We used a coronagraphic mask with a $0.6''$ diameter to suppress the brightness of GG Tau Aa/Ab. We obtained 64 frames with an exposure time of 30 s for each. We also took short exposure frames without the coronagraphic mask. For a PSF reference star, we took SAO 76661 after the GG Tau observations with the same instrumental configuration except when using the $0.3''$ diameter coronagraphic mask. We used a neutral density filter in the AO system to match the R -band magnitudes between GG Tau and SAO 76661 where wavefronts were sensed. Twelve frames were taken with an exposure time of 30 s.

The Image Reduction and Analysis Facility (IRAF¹) software was used for data reduction. We followed the reduction procedures given by Tanii et al. (2012). All HiCIAO frames have artifacts of horizontal stripes and vertical bandings. These patterns were removed with a dedicated program.

¹ IRAF is distributed by National Optical Astronomy Observatory, which is operated by the Association of Universities for Research in Astronomy, Inc., under cooperative agreement with the National Science Foundation.

Next, we removed hot and bad pixels and divided the object frames by the flat frame. After these procedures were applied, we obtained flux images of the polarimetric components, F_{0° and F_{90° , F_{90° and F_{0° , F_{45° and F_{135° , and F_{135° and F_{45° , which formed separate images on the left and right sides. The Stokes parameters, Q and U , were derived as

$$Q = F_{0^\circ} - F_{90^\circ}, \quad (1)$$

$$U = F_{45^\circ} - F_{135^\circ}. \quad (2)$$

By subtracting the images on the right from the images on the left, we obtained 16 images of Q and $-Q$ and 16 images of U and $-U$. We constructed images of the intensity of polarization (PI) by

$$PI = \sqrt{Q^2 + U^2}. \quad (3)$$

Assuming that polarization due to interstellar material in front of GG Tau is negligible, the image of intensity of polarization represents the polarized components of circumbinary structures.

To derive the degree of polarization, P , of the circumbinary structures, the image of the intensity of polarization needs to be divided by the intensity image, which contains only the components of the circumbinary structures. The intensity image of GG Tau (hereafter I_{tot}) consists of the intensity of circumbinary structures as well as that of the central binary. By subtracting the intensity image of the central binary (I_*) from I_{tot} , we obtained an intensity image of the circumbinary structure (I_{disk}), i.e., $I_{\text{disk}} = I_{\text{tot}} - I_*$. For I_* , we created a pseudo-binary image by duplicating the images of the PSF reference star. A detailed description of the PSF subtraction is presented in Itoh et al. (2002). Even with the procedure above, we did not subtract the PSF of the GG Tau binary perfectly. We attribute this imperfection to a mismatch between the AO corrections of GG Tau and the PSF reference star. As a result, the degrees of polarization have uncertainties as large as 20%. On the other hand, the angle of polarization and intensity of polarization are trustworthy because these two values were obtained before the PSF subtraction was applied.

3 RESULTS AND DISCUSSION

The image of intensity of polarization for the GG Tau A binary is shown in Figure 1 with the polarization vectors overlaid. The central binary was imaged within the coronagraphic mask which significantly suppressed light. The ring-shaped circumbinary disk is clearly seen. The degrees of polarization for the circumbinary disk are between 30% and 100%.

The gap structure in the circumbinary disk is evident as a sudden dip to the west. We propose three hypotheses for this structure: a less dense region around a planet, a shaded region formed by the circumbinary structure or a shadow cast by the inner material. Numerical simulations indicate that in an early phase of planetary formation, a less dense region appears around a planet (e.g., Mayer et al. 2004). If the region is optically thin, a gap structure appears in the image of intensity of polarization for the disk. The less dense region around a planet would orbit the binary with a Keplerian velocity.

We detected the orbital motion of the gap structure by comparing the image taken in 2001 (Itoh et al. 2002) with the one taken in 2011. Because the inclination of the disk is 37° , the positions of the gap structure were measured in the deprojected disk. We defined a box as the gap region, for which two short sides are interpolations of the inner and outer edges of the circumbinary disk. Points at the intersections of these two sides with the middle of the long sides are defined as the reference points of the gap structure. The positions of the reference points are measured from the centroid of the binary. The mass of each component of the binary is $0.78 M_\odot$ and $0.68 M_\odot$, respectively (White et al. 1999). The positions of the binary components are accurately measured in the image from 2001, because the coronagraphic mask has a transmittance of a few tenths of a percent. For the image from 2011, the positions of the binary are measured in the short exposure frames. The separations between the centroid of the binary and the inner reference point of the gap structure were 150 AU

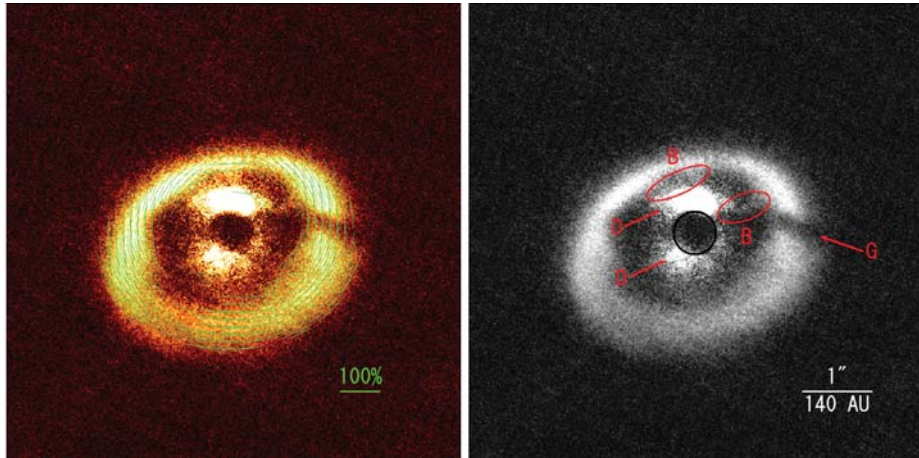


Fig. 1 (left) An H -band image of polarization intensity for the GG Tau Aa/Ab binary system. Polarization vectors are overplotted. Degrees and angles of the polarization in an 11×11 pixel box are averaged, if the intensity of polarization is detected to more than 6σ above the sky background and if the degree of each pixel is less than 100%. The field of view is $6.5'' \times 6.5''$. North is up and east is toward the left. (right) Structures discussed below are indicated on the intensity of polarization. G: the gap structure, D: the circumstellar disks and B: the bridges. The black circle indicates the position of the coronagraphic mask.

in 2001 and 160 AU in 2011. Those of the outer reference point were 240 AU in 2001 and 260 AU in 2011. We consider that these discrepancies are due to ambiguous boundaries of the gap region. The position angle (PA) of the inner reference point was -91.5° in 2001 and -85.6° in 2011. That of the outer reference point was -101.4° in 2001 and -96.5° in 2011. Changes in the PAs are $+5.9^\circ$ for the inner reference point and $+4.9^\circ$ for the outer reference point. These changes correspond to orbital periods of 650 yr and 780 yr, respectively, assuming a constant angular velocity. However, the expected orbital periods are 1700 yr for a point at 160 AU from the centroid and 3500 yr for a point at 260 AU. The change in the PA during two observational epochs should be 2.2° and 1.1° for the inner and outer reference points, respectively. Thus, the change in the PAs of the gap is not consistent with the angular velocity predicted from the Kepler motion of the circumbinary disk.

Moreover, the motion of the gap structure is in a direction opposite to that of the disk material. Kawabe et al. (1993) resolved the circumbinary disk in millimeter wavelengths. The redshifted component of the ^{12}CO emission is located to the west of the dust continuum and the blueshifted component to the east. Roddier et al. (1996) observed the GG Tau binary in near-infrared wavelengths with an AO system. They revealed the orbital motions of the binary components are in the clockwise direction. Assuming that the orbital angular momenta of the stars and the circumbinary disks are roughly in the same direction, Guilloteau et al. (1999) indicated that the material in the circumbinary disk orbits in the clockwise direction and the disk is inclined such that its northern edge is nearest to us. On the other hand, comparison of the optical and near-infrared images of GG Tau reveals that the gap structure moves in the opposite direction. In the HST optical image taken in 1997, the PA of the gap is -92° (Krist et al. 2002). In the near-infrared image taken in 1998 with HST (Silber et al. 2000) and in that taken in 2001 with the Gemini telescope (Potter et al. 2001), the PAs of the gap structure seem to be around -90° . In the near-infrared image taken in 2001, the PA of the gap structure is -91.5° at the inner reference point and -101.4° at the outer reference point

(Itoh et al. 2002). The PAs of the gap structure are -85.6° at the inner reference point and -96.5° at the outer reference point in 2011. These measurements indicate that the motion of the gap structure is counterclockwise and in a direction opposite that of the disk material. We conclude that the gap structure is not a less dense region around a planet in the circumbinary disk.

Next, we consider a shaded region formed by the circumbinary structure. It is expected that the shaded region appears as a dark area in the image of intensity of polarization for the disk, if the disk has a local concave structure. If the circumbinary disk is a rigid body, a local concave structure, and thus a shaded region, would orbit the binary in a prograde direction. Otherwise, if a retrograde density wave propagates through the circumbinary disk, the shaded region moves independently of the disk's matter. However, spiral density waves in a circumstellar disk can be amplified only if the wave rotates in a prograde sense (e.g. Shu et al. 2000). We claim that the gap structure is not a shaded region made by a local concave structure in the circumbinary disk.

Itoh et al. (2002) proposed that the gap structure may be a shadow caused by the material between the central binary and the circumbinary disk. First, we consider a circumstellar disk of the binary component to be an obscuring structure. It is known that the circumbinary disk is a thick flared disk. If the circumstellar disk is largely inclined with respect to the plane of the circumbinary disk; illumination from the central star on the circumbinary disk would be suppressed along the midplane of the circumstellar disk. However, Silber et al. (2000) rejected this hypothesis due to the lack of a second, diametrically opposed gap on the circumbinary disk. Krist et al. (2002) proposed a circumstellar disk with a large azimuthal density enhancement. Such an enhancement may project a shadow on the circumbinary disk to produce the gap structure. The PA of the gap axis should equal the PA of the gap structure, if an obscuring structure is spherical or extends only in the radial direction. However, the PA of the gap axis is -111° , which is very different from the PA of the gap structure. If the obscuring structure extends in the azimuthal direction, the structure can create a shadow whose axis PA is different from the PA of the shadow. A circumstellar disk with an azimuthal density enhancement has been reported around several YSOs (e.g. AB Aur, Fukagawa et al. 2004; V718 Per, Grinin et al. 2008). The gap structure moves in a retrograde direction. Assuming that the orbital angular momenta of the stars, the circumstellar disks and the circumbinary disks are roughly in the same direction, a precessing circumstellar disk may account for the shadow. Such a disk is proposed for the circumbinary disk around an eclipsing young system, KH 15D (Kusakabe et al. 2005). As a conclusion, we propose that there is a precessing circumstellar disk with an azimuthal structure, casting a shadow on part of the circumbinary disk.

As the obscuring structure other than the circumstellar disk, Krist et al. (2002) proposed that there is a dense clump in an accretion stream. We also imagine that the jet emanating from the secondary star tilts toward the circumbinary disk. Dust in the jet blocks a part of the light from the primary star, making a shadow on the circumbinary disk. To identify the obscuring structure, high-spatial resolution observations in the close vicinity of the binary system are required.

There are emissions between the binary and the circumbinary disk. Two emissions around the binary extend north and south. Bridge structures are seen with PA between 0° and 40° and with PA at -60° , respectively. These structures are not ghosts, because these are polarized. If they were not polarized, no structure would appear in the image of intensity of polarization. The polarization vectors depicted in part of the structures face the binary, indicating scattering is occurring. We consider that the former and latter structures correspond to the circumstellar disks and bridges between the circumbinary disk and the circumstellar disks, respectively. A bridge structure between a circumbinary disk and circumstellar disks is suggested in many numerical simulations (e.g. Bate & Bonnell 1997; Hanawa et al. 2010). Materials in a circumbinary disk are thought to accrete to circumstellar disks through the bridge structure. The northern bridge may correspond to the millimeter dust streamer (Piétu et al. 2011). However, because of the imperfection arising from the PSF subtraction, detections of these structures are marginal. Further polarimetric observations are required under stable conditions.

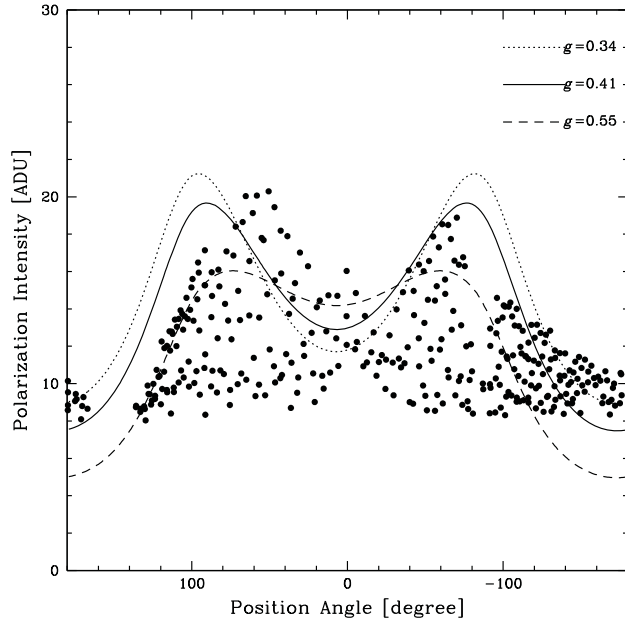


Fig. 2 An azimuthal profile of the intensity of polarization for the circumbinary disk of GG Tau. The intensities of polarization in an 11×11 pixel box are averaged, if the intensity of polarization is detected to more than 6σ above the sky background and if the degree of polarization for each pixel is less than 100%. With this detection threshold, the polarization vectors cover most of the region of the circumbinary disk (see Fig. 1). Intensities of polarization derived from a simple disk model are shown by lines.

Figure 2 shows the azimuthal profile of the H -band intensity of polarization for the circumbinary disk. In the figure, the intensities of polarization derived with a simple disk model are also shown. The profile of the intensity of polarization is a combination of an intensity profile and a profile of the degree of polarization. We used the Henyey-Greenstein phase function and the Rayleigh function (White 1979). We employed the disk model proposed by Guilloteau et al. (1999), i.e. the inclination of the disk is 37° , the PA of the semiminor axis is 7° and the disk opening angle is 15° . From intensity profiles of the disk in multi-wavelengths, Duchêne et al. (2004) derived the scattering parameter g of the Henyey-Greenstein phase function to be 0.41 for the best fit and 0.34–0.55 for acceptable values. We calculated the polarized intensities with $g = 0.34$, 0.41 and 0.55. The polarized intensity will decrease, if the disk surface ripples for example. We compared the polarized intensity derived from the disk model with the maximum of the observed polarized intensity at each position angle. Among the three models, the model with $g = 0.41$ shows the best fit to the observed polarized intensity. Because the disk is optically thick in the H -band, light from the central star is scattered in the surface of the disk. The observed polarized intensity profile is well reproduced with Rayleigh-like scattering, indicating there are small particles in the surface layer. Duchêne et al. (2004) proposed a stratified structure, which claimed that large dust grains settled in the midplane of the disk, and the disk surface is dominated by small dust grains. The azimuthal profile of the observed polarized intensity of the disk is consistent with this two-layer structure. Nevertheless, the discrepancies in the polarized intensity between the observation and the model are rather large. We attribute this mismatch to the

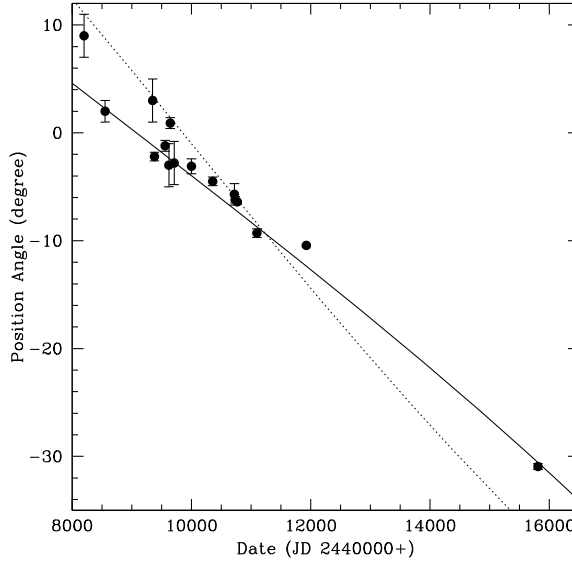


Fig. 3 PAs of the central binary. The filled circles represent the observed PAs. The solid line indicates the PAs for the orbit with $a = 33.4$ AU and $e = 0.34$. The dotted line indicates the PAs for the orbit with $a = 62$ AU and $e = 0.35$.

use of a simple model. Comparison of the degree of polarization between observations and the 3-D disk model with light scattering from non-spherical dusts will reveal the distribution of dust size in the circumbinary disk.

The orbital motion of the central binary was also examined. The separation and PA of the binary in 2011 was 256.0 ± 1.6 mas and $-30.9^\circ \pm 0.3^\circ$ in the projected plane. The separation has been almost constant for 20 yr.

Figure 3 shows the PAs of the binary in the last 20 yr. Beust & Dutrey (2005) proposed two orbits for the binary. The small orbit has $a = 33.4$ AU and $e = 0.34$. The large orbit has $a = 62$ AU and $e = 0.35$. The expected PAs for these two orbits are also shown in Figure 3. For the large orbit, the projected separation is as large as 288 mas even at periastron. For this orbit, we draw the PAs such that the companion passed the periastron at JD = 2 450 000 (circa 1995). The PA observed in 2011 is consistent with a small orbit, but is not consistent with a large orbit. Beust & Dutrey (2005) and Beust & Dutrey (2006) pointed out that the inner edge of the circumbinary disk is approximately twice as large as should be expected with a small binary orbit. As a cause of this mismatch, they proposed that there is secular evolution in the GG Tau A orbit and a massive circumbinary planet around ~ 140 AU from the GG Tau A binary.

4 CONCLUSIONS

A high angular resolution near-infrared image that shows the intensity of polarization for the GG Tau A binary system was obtained with the Subaru Telescope.

- (1) The image shows the circumbinary disk scattering the light from the central binary. Combined with a previous observation of the circumbinary disk, our image indicates that the gap structure in the circumbinary disk orbits in the counterclockwise direction. On the other hand, material

in the disk orbits in the clockwise direction. We conclude that the gap structure is neither a less dense region around a circumbinary planet, nor a shaded region made by a local concave structure in the disk, but rather a shadow cast by the material located between the binary and the circumbinary disk.

- (2) The azimuthal profile of the intensity of polarization for the circumbinary disk is roughly reproduced by a simple disk model with the Henyey-Greenstein phase function and the Rayleigh function, indicating there are small dust grains at the surface of the disk.
- (3) The separations and PAs of the stellar components of the binary in the past 20 yr are consistent with the binary orbit with $a = 33.4$ AU and $e = 0.34$.

Acknowledgements We thank Dr. Michihiro Takami for a useful discussion. Y. I. is supported by a Grant-in-Aid for Scientific Research (No. 24540231). J. C. is supported by the U.S. National Science Foundation under Award (No. 1009203).

References

Artymowicz, P., & Lubow, S. H. 1996, *ApJ*, 467, L77
 Bate, M. R., & Bonnell, I. A. 1997, *MNRAS*, 285, 33
 Beust, H., & Dutrey, A. 2005, *A&A*, 439, 585
 Beust, H., & Dutrey, A. 2006, *A&A*, 446, 137
 Duchêne, G., McCabe, C., Ghez, A. M., & Macintosh, B. A. 2004, *ApJ*, 606, 969
 Fukagawa, M., Hayashi, M., Tamura, M., et al. 2004, *ApJ*, 605, L53
 Ghez, A. M., Neugebauer, G., & Matthews, K. 1993, *AJ*, 106, 2005
 Grinin, V., Stempels, H. C., Gahm, G. F., et al. 2008, *A&A*, 489, 1233
 Guilloteau, S., Dutrey, A., & Simon, M. 1999, *A&A*, 348, 570
 Hanawa, T., Ochi, Y., & Ando, K. 2010, *ApJ*, 708, 485
 Hioki, T., Itoh, Y., Oasa, Y., et al. 2007, *AJ*, 134, 880
 Hioki, T., Itoh, Y., Oasa, Y., Fukagawa, M., & Hayashi, M. 2011, *PASJ*, 63, 543
 Itoh, Y., Tamura, M., Hayashi, S. S., et al. 2002, *PASJ*, 54, 963
 Kawabe, R., Ishiguro, M., Omodaka, T., Kitamura, Y., & Miyama, S. M. 1993, *ApJ*, 404, L63
 Krist, J. E., Stapelfeldt, K. R., & Watson, A. M. 2002, *ApJ*, 570, 785
 Kusakabe, N., Tamura, M., Nakajima, Y., et al. 2005, *ApJ*, 632, L139
 Leinert, C., Zinnecker, H., Weitzel, N., et al. 1993, *A&A*, 278, 129
 Mayer, L., Quinn, T., Wadsley, J., & Stadel, J. 2004, *ApJ*, 609, 1045
 Piétu, V., Gueth, F., Hily-Blant, P., Schuster, K.-F., & Pety, J. 2011, *A&A*, 528, A81
 Potter, D., Baudoz, P., Guyon, O., et al. 2001, in American Astronomical Society Meeting Abstracts #198, *Bulletin of the American Astronomical Society*, 33, 812
 Roddier, C., Roddier, F., Northcott, M. J., Graves, J. E., & Jim, K. 1996, *ApJ*, 463, 326
 Shu, F. H., Laughlin, G., Lizano, S., & Galli, D. 2000, *ApJ*, 535, 190
 Silber, J., Gledhill, T., Duchêne, G., & Ménard, F. 2000, *ApJ*, 536, L89
 Tanii, R., Itoh, Y., Kudo, T., et al. 2012, *PASJ*, 64, 124
 White, R. J., Ghez, A. M., Reid, I. N., & Schultz, G. 1999, *ApJ*, 520, 811
 White, R. L. 1979, *ApJ*, 229, 954